

**Widespread seismicity excitation throughout central Japan following
the 2011 M=9.0 Tohoku earthquake, and its interpretation
by Coulomb stress transfer**

Shinji Toda¹, Ross S. Stein², Jian Lin³

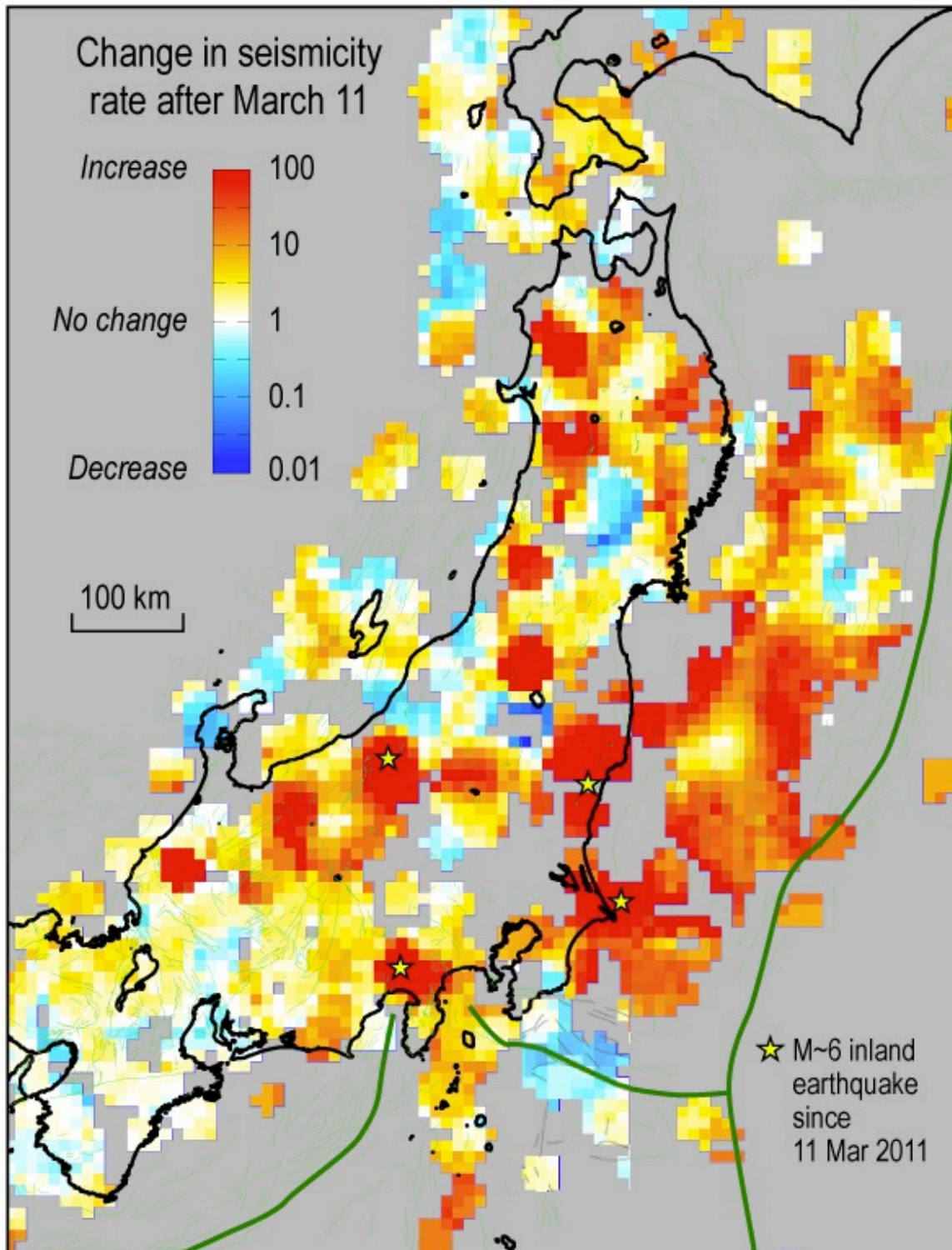
¹Disaster Prevention Research Institute, Kyoto University, Japan
toda@rcep.dpri.kyoto-u.ac.jp

²U.S. Geological Survey, Menlo Park, California, USA
rstein@usgs.gov

³Woods Hole Oceanographic Institution, Woods Hole, Massachusetts, USA
jlin@whoi.edu

Plain English Summary

We report on a broad and unprecedented increase in seismicity rate for microearthquakes ($M \geq 2$) over a broad 600 by 200 km (360 by 120 mi) area across inland Japan, parts of the Japan Sea and the Izu islands, following the M=9.0 Tohoku mainshock. The seismicity increase occurs at distances of up to 425 km (360 mi) from the region of high (≥ 15 m or 50 ft) seismic slip on the megathrust rupture surface of the M=9 earthquake. Are these aftershocks, and if so what do they signify for the likelihood of large earthquakes across this region? While the origin and implications of the seismicity increase is subject to debate, its occurrence is beyond dispute. It was not seen for the 2004 M=9.1 Sumatra and 2010 M=8.8 Chile earthquakes, but they lacked the seismic networks necessary to detect such small events. Here we explore the possibility that the rate changes are the product of static or permanent stress transfer from the mainshock to small surrounding faults. We find that half of the areas we can examine show a positive association between calculated stress changes and the observed seismicity rate change, three show a negative association, and in four show changes too small to assess. Regardless of the process that promotes the aftershocks, we argue that the microseismicity increases demonstrate that the ‘remote’ inland Japan and Japan Sea and shocks (e.g., the Nagano Mw=6.3 on 3/12 03:59, the Japan Sea Mw=6.2 on 3/12 04:46, the Mt. Fuji Mw=5.8 on 3/15, 22:31) are not exceptional; in fact they are not truly isolated events. Instead, they simply represent the largest shocks in a very broad zone of elevated seismicity rate that is evident for $M \geq 2$ earthquakes.



1 Widespread seismicity excitation throughout central Japan 2 following the 2011 M=9.0 Tohoku earthquake 3 and its interpretation by Coulomb stress transfer

4 Shinji Toda,¹ Ross S. Stein,² and Jian Lin³

5 Received 24 April 2011; revised 22 June 2011; accepted 28 June 2011; published XX Month 2011.

6 [1] We report on a broad and unprecedented increase in
7 seismicity rate following the M=9.0 Tohoku mainshock
8 for $M \geq 2$ earthquakes over inland Japan, parts of the Japan
9 Sea and Izu islands, at distances of up to 425 km from the
10 locus of high (≥ 15 m) seismic slip on the megathrust. Such
11 an increase was not seen for the 2004 M=9.1 Sumatra or
12 2010 M=8.8 Chile earthquakes, but they lacked the seismic
13 networks necessary to detect such small events. Here we
14 explore the possibility that the rate changes are the product
15 of static Coulomb stress transfer to small faults. We use the
16 nodal planes of $M \geq 3.5$ earthquakes as proxies for such
17 small active faults, and find that of fifteen regions averaging
18 ~ 80 by 80 km in size, 11 show a positive association
19 between calculated stress changes and the observed seismic-
20 ity rate change, 3 show a negative correlation, and for one the
21 changes are too small to assess. This work demonstrates that
22 seismicity can turn on in the nominal stress shadow of a main-
23 shock as long as small geometrically diverse active faults
24 exist there, which is likely quite common. **Citation:** Toda, S.,
25 R. S. Stein, and J. Lin (2011), Widespread seismicity excitation
26 throughout central Japan following the 2011 M=9.0 Tohoku earth-
27 quake and its interpretation by Coulomb stress transfer, *Geophys.*
28 *Res. Lett.*, 38, LXXXXX, doi:10.1029/2011GL047834.

29 1. Introduction

30 [2] The M=9.0 Tohoku-chiho Taiheiyo (hereafter,
31 'Tohoku') earthquake resulted from slip on a roughly 500-
32 km-long and 200-km-wide seismic megathrust source
33 ([http://tectonics.caltech.edu/slip_history/2011_taiheiyo-oki/
34 index.html](http://tectonics.caltech.edu/slip_history/2011_taiheiyo-oki/index.html)). Many offshore aftershocks, including four
35 $M \geq 7$ and ~ 70 $M \geq 6$ shocks, have struck during the ensuing
36 three months. The possibility of other large earthquakes on
37 adjacent portions of the megathrust, similar to the 28 March
38 2005 M=8.6 Simeulue-Nias earthquake following the
39 26 December 2004 M=9.1 Sumatra-Andaman earthquake
40 [Nalbant *et al.*, 2005; Pollitz *et al.*, 2006] are thus possible.
41 Sites of potential tsunamigenic earthquakes include the
42 Sanriku-Hokubu area to the north, and Off-Boso (east of the
43 Boso peninsula) to the south [Headquarters for Earthquake
44 Research Promotion, 2005] of the 2011 Tohoku rupture.
45 [3] Equally important for the exposed population and
46 infrastructure would be the occurrence of large inland shocks

in northern Honshu. Three $M \sim 6$ shallow inland earthquakes 55
have struck as far as ~ 300 km from the M=9 source since the 56
Tohoku mainshock, reaffirming the broad reach and trig- 57
gering potential of the great quake (Figure 1a). The 11 58
April 2011 Mw=6.7 Iwaki earthquake produced 40 km of 59
normal faulting, with a peak surface slip of 2 m. Among 60
such inland sites, none is more important than Tokyo, which 61
was last struck by the 1923 Kanto M=7.9 Sagami mega- 62
thrust event [Nyst *et al.*, 2006], and a deeper inland event in 63
the 1855 $M \sim 7.2$ Ansei-Edo earthquake [Grunewald and 64
Stein, 2006]. This concern is heightened by several inland 65
large earthquakes in Tohoku that have followed M=7–8 inter- 66
plate events by months to a decade [Shimazaki, 1978; Seno, 67
1979; Churei, 2002], including the 31 August 1896 Mj = 7.2 68
Rikuu earthquake, which produced a 30-km-long surface 69
rupture that devastated the eastern Akita Prefecture, with 70
200 deaths (Figure 2a). 71

[4] To evaluate the potential triggering impact of the 72
Tohoku earthquake to inland Japan, we analyze the seis- 73
micity rate change since the Tohoku mainshock, and cal- 74
culate the associated static Coulomb stress changes over the 75
region of seismicity rate change. 76

2. Inland Seismicity Rate Changes Associated 77 With the Tohoku Earthquake 78

[5] The widespread seismicity rate increase across central 79
Japan and extending west to the Japan Sea and south to the 80
Izu islands is evident in Figure 1. Broadly, there are strong 81
increases in seismicity rate across a region extending up to 82
300 km from the distal edges of the M=9 rupture surface, 83
and 425 km from the locus of high (≥ 15 m) seismic slip. In 84
addition to the microseismicity, an Mj=6.7 earthquake 85
occurred 13 hours after the Tohoku mainshock in box N, a 86
Mj=6.4 earthquake occurred 24 hours after the Tohoku 87
earthquake in box A, and a Mj=6.4 earthquake struck about 88
4.5 days after the Tohoku earthquake at the base of Mt. Fuji 89
(just west of box R). While it might appear that these remote 90
earthquakes are distinct from aftershocks closer to the rup- 91
ture plane, Figure 1 suggests that it is more likely that they 92
are simply the largest events to occur within the zone of 93
increased seismicity rate. 94

[6] Remote earthquake triggering was observed at even 95
greater distances but much lower densities following the 1992 96
M=7.3 Landers and 2002 M=7.9 Denali, earthquakes [Hill, 97
2008]. Nevertheless, the broad seismic excitation for Tohoku 98
is unprecedented, although for the roughly-equivalent 2004 99
M=9.1 Sumatra, Indonesia, and 2010 M=8.8 Maule, Chile, 100
earthquakes, no $M < 4.7$ aftershock could be detected. 101

[7] Sudden increases of post-Tohoku seismicity are observed 102
in regions B (Akita), J (southern Fukushima – northern Ibaraki), 103

¹Disaster Prevention Research Institute, Kyoto University, Kyoto, Japan.

²U.S. Geological Survey, Menlo Park, California, USA.

³Woods Hole Oceanographic Institution, Woods Hole, Massachusetts, USA.

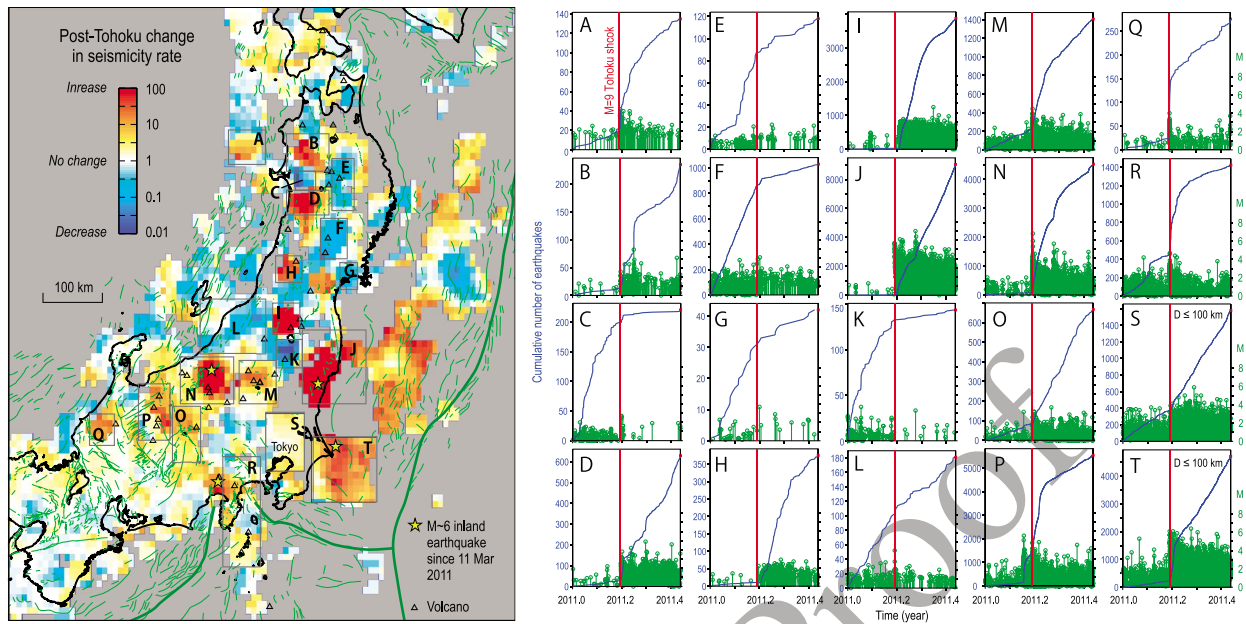


Figure 1. (left) Seismic response of inland Japan to the M=9.0 Tohoku mainshock for M ≥ 1.0 seismicity (90 days post-mainshock compared to 1.2-year pre-mainshock), with a smoothing radius of 20 km, using the JMA PDE catalog downloaded on 10 June 2011. M_c is based on *Nanjo et al.* [2010] for inland Japan; M_c could be ~2.0 post-11 March 2011. Except for S and T (0–100 km), all boxes use earthquakes at 0–20 km depth. Dark green lines show plate boundaries. (right) Time series for the boxed regions show cumulative numbers of $M_j \geq 0.0$ earthquakes during 1/1–6/10/2011 (blue); each earthquake is shown as a green stem proportional to JMA magnitude, M .

104 T (Cape Inubou), M (Mt. Hotaka–Mt. Asahi), S (Kanto),
 105 where a burst of seismicity began at the head of Tokyo Bay
 106 several days after the Tohoku shock, R (Izu and islands), and
 107 P (Hida mountain range) (Figure 1). An increase in seismicity
 108 rate apparently delayed by 1–3 days is observed in the box I.
 109 The increase in seismicity in regions N and A could be
 110 masked by aftershocks of the M ~ 6 mainshocks, or the larger
 111 events could be part of the same process. The JMA (Japan
 112 Meteorological Agency) PDE catalog normally lists earth-
 113 quakes that have occurred until two days before present, but
 114 because of the enormous number of aftershocks, seismic
 115 station damage and power outages, there is some chance that
 116 the seismicity rate drops in boxes C, E, F, G, K, and L might
 117 be data lapse artifacts. In contrast, the sudden seismicity rate
 118 jumps are likely real. Some of the rate increases (boxes A, H,
 119 I, M, N, P, Q, and R) exhibit gradual declines since March 11
 120 reminiscent of aftershock sequences, whereas others exhibit a
 121 continuous high rate (boxes D, J, O, S, and T).

122 3. Calculation of the Coulomb Stress Change

123 [8] The static Coulomb stress change caused by a main-
 124 shock has been widely applied to assess areas of subsequent
 125 off-fault aftershocks [e.g., *Reasenber and Simpson*, 1992].
 126 The Coulomb stress change is defined as $\Delta CFF = \Delta\tau +$
 127 $\mu\Delta\sigma$, where τ is the shear stress on the fault (positive in the
 128 inferred direction of slip), σ is the normal stress (positive for

129 fault unclamping), and μ is the apparent friction coefficient. 129
 Failure is promoted if ΔCFF is positive and inhibited if 130
 negative; both increased shear and unclamping of faults are 131
 taken to promote failure, with the influence of unclamping 132
 controlled by fault friction. 133

[9] To resolve the Coulomb stress change on a ‘receiver 134
 fault’ (fault receiving stress from a mainshock) requires a 135
 source model of the earthquake fault slip, as well as the 136
 geometry and slip direction on the receiver. One can assume 137
 that the receiver faults share the same strike, dip and rake as 138
 the mainshock source fault, one can resolve stress on a major 139
 fault of known geometry [e.g., *McCloskey et al.*, 2003], or 140
 one can find the receiver faults at every point that maximize 141
 the Coulomb stress increase given the earthquake stress 142
 change and the tectonic stress [*King et al.*, 1994], termed the 143
 ‘optimally-oriented’ Coulomb stress change. However, the 144
 M=9.0 Tohoku earthquake at least temporarily raised the 145
 seismicity rate across a region so large that thrust, normal 146
 and strike-slip faults co-exist in tectonic stress fields asso- 147
 ciated with the complex convergence of three tectonic 148
 plates. One solution is to resolve the stress change on major 149
 active faults [*Toda et al.*, 2011] based on their inferred 150
 geometry and slip sense. While this is instructive as a guide 151
 to the likelihood that one of these major faults could rupture, 152
 the faulting mechanisms of small to moderate shocks that 153
 dominate the local seismicity increase are undoubtedly more 154

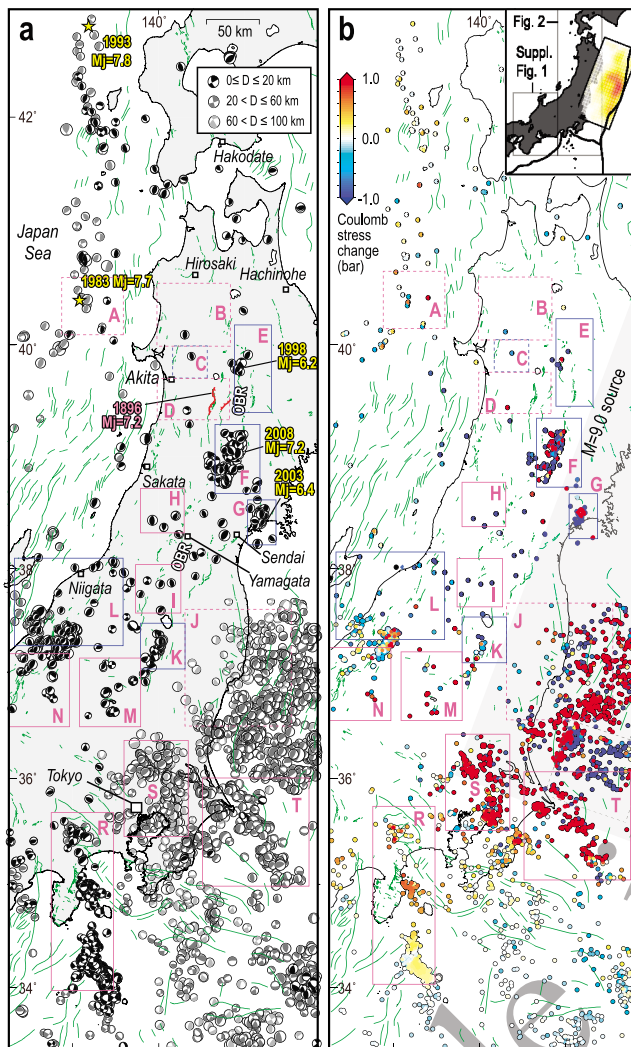


Figure 2. Coulomb stress changes resolved on the nodal planes of small earthquakes as proxies for small active faults. (a) Focal mechanisms from the F-net catalog (<http://www.fnet.bosai.go.jp/top.php?LANG=en>) since 1997 (depth ≤ 20 km for inland areas, ≤ 50 km for the eastern margin of Japan Sea region, and ≤ 100 km for Kanto); D is depth. (b) Maximum Coulomb stress change from each pair of nodal planes; where earthquakes overlap, the most positively-stressed shocks are plotted on top. The color of the box boundaries indicates the overall seismicity change inside each box: Increase (red) and decrease (blue). Dashed boxes show regions that are not shown in Table 1 for reasons discussed in the text.

155 complex and varied than the associated major structures, and
156 so here we propose an alternative.

157 4. Use of Focal Mechanisms as Proxies for Small 158 Active Faults

159 [10] We instead resolve the Coulomb stress changes on
160 the nodal planes of the abundant small earthquakes as
161 proxies for active faults. If the earthquake-induced stress
162 field fundamentally changes the kinds of quakes that can be
163 triggered, this method will fail, as it does at the site of the
164 $M=6.7$ Iwaki tensional earthquake that produced 40 km of

surface normal faulting in a region that was formerly dom- 165
166 inated by thrust events. But we will show that most pre-
167 Tohoku mechanisms are consistent with stress transfer to the
168 aftershocks, and that further, the diversity of the pre-Tohoku
169 mechanisms is much greater than that associated with the
170 major surface faults, and so is more representative of the
171 aftershock faulting.

[11] We make use of fault plane solutions of the full, 172
14-year-long F-net catalog (<http://www.fnet.bosai.go.jp/top.php?LANG=en>), which for inland Japan principally 173
includes shallow crustal earthquakes of $M_j \geq 3.5$; this corre- 174
sponds to source dimension ≥ 400 m [Wells and Coppersmith, 175
1994]. Even though mapped faults [Research Group for 176
Active Faults in Japan, 1991] often have sinuous and en 177
echelon traces, comparison of the faults (green lines) with the 178
focal mechanisms in Figure 2a and Figure S1a of the auxiliary 179
material, reveals that the mechanisms exhibit even more 180
complexity, such as strike-slip faults amid the mapped thrust 181
faults of Tohoku, or thrust mechanisms with a wide range of 182
strikes at the site of the 2008 $M_j=7.2$ Iwate-Miyagi Nairiku 183
earthquake (Figure 2a, box F). 184
185

[12] Toda *et al.* [2011] tested six representative source 186
models and three friction values (0.0, 0.4, and 0.8) to 187
determine the model producing the greatest gain in after- 188
shock mechanisms that are promoted by the mainshock, 189
relative to the promotion of the background (pre-Tohoku) 190
mechanisms, which serves as a control population. This was 191
the most rigorous test possible of the Coulomb failure 192
hypothesis that could be applied to the 2011 Tohoku 193
aftershock sequence less than one month after the mainshock. 194
The Wei *et al.* source model (http://tectonics.caltech.edu/slip_history/2011_taiheiyo-oki/index.html) and a friction of 195
0.4 produced the greatest (62%) gain, which we use here to 196
calculate the stress changes in an elastic half space with 197
Poisson's ratio 0.25 and shear's modulus 3.2×10^5 bar, 198
using Coulomb 3.3 (www.coulombstress.org). We resolve 199
the static Coulomb stress change on both nodal planes at 200
each hypocenter because we do not know which of the two 201
nodal planes slipped. In Figures 2b and S3b of the auxiliary 202
material, we plot the maximum Coulomb stress change for 203
the most positive plane only (we would otherwise have to 204
plot both sets of planes), and also place positive changes 205
(red dots) atop negative changes (blue dots) where earth- 206
quakes overlap. Thus, the figures have an intentional 'red 207
bias,' but Table 1 uses both nodal planes and has no bias. 208
209

210 5. Comparison of Seismicity Rate Changes 211 and Coulomb Stress Changes

[13] Comparison of Figure 1 with Figures 2b and S3b of 212
the auxiliary material indicates positive associations between 213
observed seismicity rate increases (i.e., aftershocks) and 214
Coulomb stress increases resolved on nodal planes in 11 of 215
the 15 boxes. We find no clear change stress in one box 216
(Q, Table 1), and negative correlations, which contradict our 217
hypothesis, in 3 boxes (H, I and N). Thus in general, slip on 218
small faults that are revealed by the background focal 219
mechanisms was promoted by the 2011 rupture even when 220
slip on the major faults, as represented by the surface trace 221
and geometry, was inhibited. This means that associated 222

¹Auxiliary materials are available in the HTML. doi:10.1029/2011GL047834.

tl.1 **Table 1.** The Percentage of Nodal Planes That Experienced a Calculated Coulomb Stress Increase and Average Coulomb Stress Change
 tl.2 Compared With the Observed Seismicity Rate Change^a

tl.3	Box From	Minimum	Maximum	Minimum	Maximum	Positive	Average	Seismicity	Correlation Between
tl.4	Figure 1 ^b	Longitude (deg)	Longitude (deg)	Latitude (deg)	Latitude (deg)	ΔCFF^c (%)	ΔCFF (bar)	Rate Change	Rate Change and ΔCFF
tl.5	E	140.85	141.27	39.42	40.29	7	-1.8	Decrease	Positive
tl.6	F	140.64	141.14	38.70	39.30	12	-3.3	Decrease	Positive
tl.7	G	141.00	141.34	38.24	38.64	10	-7.7	Decrease	Positive
tl.8	H	139.79	140.29	38.34	38.74	0	-3.2	Increase	Negative
tl.9	I	139.74	140.25	37.55	38.00	0	-2.3	Increase	Negative
tl.10	K	139.80	140.30	37.04	37.46	13	-1.3	Decrease	Positive
tl.11	L	138.37	139.61	37.25	38.06	17	-0.6	Decrease	Positive
tl.12	M	139.10	139.80	36.50	37.15	59	0.6	Increase	Positive
tl.13	N	138.00	139.00	36.50	37.20	15	-0.4	Increase	Negative
tl.14	O	137.85	138.38	35.61	36.46	62	0.2	Increase	Positive
tl.15	P	137.20	137.80	35.95	36.80	87	0.3	Increase	Positive
tl.16	Q	136.29	136.76	35.88	36.36	44	0.004	Increase	(Negative)
tl.17	R	138.80	139.50	34.00	35.70	82	0.11	Increase	Positive
tl.18	S	139.61	140.33	35.48	36.37	83	1.2	Increase	Positive
tl.19	T	140.50	141.70	35.00	36.00	75	2.5	Increase	Positive

tl.20 ^aThere are two for each earthquake. Because of the preliminary state of the aftershock catalog, the correlations are approximate.

tl.21 ^bBoxes with less than 10 focal mechanisms excluded.

tl.22 ^c ΔCFF = Coulomb stress change; ΔCFF positive $\geq 50\%$ (red); $<50\%$ (blue). Ave. ΔCFF value ≥ 0 (red); <0 (blue).

223 with the major faults are many secondary features, such as
 224 ramps, tears, echelons, splays, and antithetical faults, which
 225 can be the sites of aftershocks that are triggered by the
 226 mainshock rupture even when slip on the major faults is
 227 inhibited.

228 [14] The positive correlations include boxes T and S
 229 straddling the rupture, box R located 150–225 km from the
 230 rupture surface, and box P, 250 km from the rupture edge. In
 231 box S (Kanto district), we included mechanisms as deep as
 232 100 km because of the complex plate configuration beneath
 233 Tokyo [Toda *et al.*, 2008]. More than 80% of the stress
 234 changes for mid to deeper shocks along the NS-trending
 235 ‘Kanto seismic corridor’ (box S) are positive (Figure 2b).

236 [15] There is also a correlation between the (albeit pre-
 237 liminary) seismicity rate decreases and stress decreases in
 238 boxes E, F, G, K, and L. Detecting seismicity rate decreases
 239 normally requires not only a high rate of preceding seis-
 240 micity, but also a long post-mainshock catalog that is not yet
 241 available. Box F was the site of the 2008 M_j=7.2 Iwate-
 242 Miyagi Nairiku earthquake; although the aftershock fre-
 243 quency would be expected to decay, there is an abrupt drop
 244 at the time of the Tohoku mainshock. The rate drops in
 245 boxes C, F, and K are very large and abrupt, and so may be
 246 real.

247 [16] Inconsistent with the static stress hypothesis, box I
 248 shows a delayed rate increase but no stress increase, and
 249 there are seismicity rate increases in box A for which
 250 Coulomb stress increases are present but do not dominate.
 251 Boxes A–D lack sufficient focal mechanisms for confident
 252 assessment. Box N, chosen to be centered on the M_j=6.7
 253 shock, shows a rate increase but a stress decrease. Box J is
 254 not analyzed because the post-Tohoku seismicity is asso-
 255 ciated with shallow normal faulting, whereas the focal data
 256 contain only deep reverse mechanisms. The boxes with a
 257 paucity of pre-Tohoku focal mechanisms (e.g., A, B, and D),
 258 and another in which the aftershock mechanisms bear no
 259 resemblance to the pre-Tohoku mechanisms (J) challenge
 260 this approach. When we resolve the Coulomb stress changes
 261 on the post-Tohoku focal mechanisms, we are able to sub-
 262 stantially increase the number of focal mechanisms for box J.

263 When we do so, we find that 93% are brought closer to
 264 Coulomb failure (Figure S3 of the auxiliary material).

265 [17] A majority of the mechanisms along the Ou backbone
 266 mountain range (boxes B, C, D, F in Figure 2b) are thought
 267 to be north-striking thrust faults, which would lie in the
 268 principal stress shadow of the Tohoku mainshock, and thus
 269 be brought farther from failure [Toda *et al.*, 2011]. How-
 270 ever, the significant percentage of strike-slip mechanisms
 271 and thrusts of divergent strikes result in a large number of
 272 positive stress changes. This underscores that resolving
 273 stress on the major faults idealizes the much more complex
 274 stress transfer.

275 [18] We also show all active volcanoes in Figure 1. There
 276 does not seem to be any overall association of seismicity
 277 rate increases with volcanic regions. Rate increases in boxes
 278 M, N, O, P and Q are at least roughly associated with vol-
 279 canoes, but so are rate decreases in boxes E, F, and K.
 280 Further, boxes O and P are associated with the Itoigawa-
 281 Shizuoka Tectonic Line (ISTL), and so it is difficult to be
 282 certain whether the transform faults or the active volcanoes
 283 are more influential.

6. Discussion and Conclusions

284 [19] The fundamental observation driving this study is the
 285 widespread seismicity rate increase across inland Japan, and
 286 extending to the Japan Sea and to the Izu island chain.
 287 Remarkably, seismicity turned on at distances of up to
 288 300 km from the lower edge of the Tohoku earthquake
 289 rupture surface, and up to 425 km from the high (<15 m) slip
 290 zone. These seismicity rate increases are apparent for $M \geq 2$
 291 earthquakes, about half the boxes include $M \geq 4$ earthquakes
 292 and in four cases include $M=5-6$ earthquakes. Most of these
 293 increases immediately follow the Tohoku mainshock, but
 294 some were delayed by up to several days. These distant
 295 aftershocks could be triggered dynamically, they could be
 296 caused by the static stress changes, or both. We note,
 297 however, that the seismicity rate changes across Japan are
 298 not well correlated with the peak ground acceleration
 299 recorded by the NIED K-Net/KiK-net strong motion net-
 300 work (Figure S2 of the auxiliary material). Although the
 301

302 ground surface acceleration is enhanced by sedimentary
303 basins, the observed seismicity rate increases and decreases
304 do not appear to be explained by shaking.

305 [20] The maximum triggering distance, less than two
306 source dimensions from the mainshock, is consistent with
307 the global absence $M \geq 5$ shocks triggered at greater dis-
308 tances [Parsons and Velasco, 2011]. Here we adapted the
309 static hypothesis to the special circumstances of triggering
310 on very small faults that are neither optimally oriented in the
311 regional stress field nor parallel to the major faults. We thus
312 use the Coulomb stress change resolved on the nodal planes
313 of the smallest earthquakes with focal mechanisms, which
314 limits us to $M \geq 3.5$ shocks, a ≥ 400 m rupture scale that at
315 least overlaps that of the aftershocks.

316 [21] A tentative examination of the observed seismicity
317 rate changes and calculated Coulomb stress changes has met
318 with promising but certainly incomplete success, since we
319 find 11 positive and 3 negative correlations (Table 1). Five
320 of the positive correlations derive from decreases both in
321 observed seismicity rate and calculated Coulomb stress, but
322 it is perhaps too soon to be confident in the seismicity rate
323 declines. Regardless of the process that promotes the after-
324 shocks, we argue that the microseismicity increases dem-
325 onstrate that the ‘remote’ Japan Sea and inland Japan shocks
326 (e.g., $M_w=6.3$ on 3/12 03:59, $M_w=6.2$ on 3/12 04:46,
327 $M_w=5.8$ on 3/15, 22:31) are neither exceptional nor truly
328 isolated events. Instead, they simply represent the largest
329 shocks in a very broad zone of elevated seismicity rate that
330 is evident for $M \geq 2$ earthquakes.

331 [22] We also find sites of profound seismicity rate drops,
332 principally in the stress shadow for thrust faulting in inland
333 Tohoku. All five of these sites exhibit calculated Coulomb
334 stress decreases imparted by the Tohoku mainshock on
335 earthquake focal mechanisms, and so they, too, are consis-
336 tent with the static stress hypothesis. Nevertheless, seismic
337 data gaps during the 3 months after the Tohoku mainshock
338 could produce rate drop artifacts, and so we maintain some
339 caution in their evaluation. In the months ahead, these rate
340 drops will be reassessed.

341 [23] One of the surprises of this work is that the effect of
342 the stress shadow expected in Tohoku for north-striking
343 thrust fault appears localized. Instead, many sites within
344 Tohoku exhibit an increased rate of seismicity. Here we find
345 that this behavior is nevertheless consistent with static
346 Coulomb stress transfer, but to smaller faults with geome-
347 tries different from the major faults, a possibility first
348 advanced by Marsan [2006]. One important question is
349 whether the activation of these smaller divergent faults
350 could trigger a large event on one of the major thrusts, as
351 might have occurred when the 15 June 1896 $M \sim 8\text{-}1/4$ off-
352 shore Sanriku earthquake was succeeded by the 31 August
353 1896 $M_j=7.2$ Rikuu inland earthquake at the same latitude
354 (Figure 2a, box D). Since the 2011 Tohoku mainshock is
355 about ten times larger than the Meiji Sanriku mainshock,
356 there could be large changes in intraplate seismicity during
357 the months to years ahead.

[24] **Acknowledgments.** We thank David Hill, Andrea Llenos, and 358
two anonymous referees for thoughtful reviews, and we are grateful to 359
JMA and NIED for the preliminary hypocenter list and focal mechanisms. 360
[25] The Editor thanks Aaron Velasco and an anonymous reviewer for 361
their assistance in evaluating this paper. 362

References

- Churei, M. (2002), Relationships between eruptions of volcanoes, inland 364
earthquakes ($M \geq 6.2$) and great tectonic earthquakes in and around 365
north-eastern Japan Island arc, *J. Geogr.*, *111*, 175–184. 366
Grunewald, E., and R. S. Stein (2006), A new 1649–1884 catalog of destruc- 367
tive earthquakes near Tokyo and implications for the long-term seismic 368
process, *J. Geophys. Res.*, *111*, B12306, doi:10.1029/2005JB004059. 369
Headquarters for Earthquake Research Promotion (2005), National Seismic 370
Hazard Maps for Japan (2005), report, 162 pp., LOCATION??. (Available 371
at <http://www.jishin.go.jp/main/index-e.html>.) 372
Hill, D. P. (2008), Dynamic stresses, Coulomb failure, and remote triggering, 373
Bull. Seismol. Soc. Am., *98*, 66–92, doi:10.1785/0120070049. 374
King, G. C. P., R. S. Stein, and J. Lin (1994), Static stress changes and the 375
triggering of earthquakes, *Bull. Seismol. Soc. Am.*, *84*, 935–953. 376
Marsan, D. (2006), Can coseismic stress variability suppress seismicity 377
shadows? Insights from a rate-and-state friction model, *J. Geophys.* 378
Res., *111*, B06305, doi:10.1029/2005JB004060. 379
McCloskey, J., S. S. Nalbant, S. Steacy, C. Nostro, O. Scotti, and D. Baumont 380
(2003), Structural constraints on the spatial distribution of aftershocks, 381
Geophys. Res. Lett., *30*(12), 1610, doi:10.1029/2003GL017225. 382
Nalbant, S. S., S. Steacy, K. Sieh, D. Natawidjaja, and J. McCloskey 383
(2005), Earthquake risk on the Sunda trench, *Nature*, *435*, 756–757, 384
doi:10.1038/nature435756a. 385
Nanjo, K. Z., T. Ishibe, H. Tsuruoka, D. Schorlemmer, Y. Ishigaki, and 386
N. Hirata (2010), Analysis of the completeness magnitude and seismic 387
network coverage of Japan, *Bull. Seismol. Soc. Am.*, *100*, 3261–3268, 388
doi:10.1785/0120100077. 389
Nyst, M., T. Nishimura, F. F. Pollitz, and W. Thatcher (2006), The 1923 390
Kanto earthquake re-evaluated using a newly augmented geodetic data 391
set, *J. Geophys. Res.*, *111*, B11306, doi:10.1029/2005JB003628. 392
Parsons, T., and A. A. Velasco (2011), Absence of remotely triggered large 393
earthquakes beyond the mainshock region, *Nat. Geosci.*, *4*, 312–316, 394
doi:10.1038/ngeo1110. 395
Pollitz, F. F., P. Banerjee, R. Burgmann, M. Hashimoto, and N. Choosakul 396
(2006), Stress changes along the Sunda trench following the 26 December 397
2004 Sumatra–Andaman and 28 March 2005 Nias earthquakes, *Geophys.* 398
Res. Lett., *33*, L06309, doi:10.1029/2005GL024558. 399
Reasenber, P. A., and R. W. Simpson (1992), Response of regional seis- 400
micity to the static stress change produced by the Loma Prieta earthquake, 401
Science, *255*, 1687–1690, doi:10.1126/science.255.5052.1687. 402
Research Group for Active Faults in Japan (1991), *Sheet Maps and Inven-* 403
tories, rev. ed., 437 pp., Univ. Tokyo Press, Tokyo. 404
Seno, T. (1979), Intraplate seismicity in Tohoku and Hokkaido and large 405
interplate earthquakes: A possibility of a large interplate earthquake off 406
the southern Sanriku coast, northern Japan, *J. Phys. Earth*, *27*, 21–51, 407
doi:10.4294/jpe1952.27.21. 408
Shimazaki, K. (1978), Correlation between intraplate seismicity and inter- 409
plate earthquakes in Tohoku, northeast Japan, *Bull. Seismol. Soc. Am.*, 410
68, 181–192. 411
Toda, S., R. S. Stein, S. H. Kirby, and S. B. Bozkurt (2008), A slab frag- 412
ment wedged under Tokyo and its tectonic and seismic implications, *Nat.* 413
Geosci., *1*, 771–776, doi:10.1038.ngeo318. 414
Toda, S., J. Lin, and R. S. Stein (2011), Using the 2011 $M=9.0$ Tohoku 415
earthquake to test the Coulomb stress triggering hypothesis and to calcu- 416
late faults brought closer to failure, *Earth Planets Space*, doi:10.5047/ 417
eps.2011.05.010, in press. 418
Wells, D. L., and K. J. Coppersmith (1994), New empirical relationships 419
among magnitude, rupture length, rupture width, rupture area, and sur- 420
face displacement, *Bull. Seismol. Soc. Am.*, *84*, 974–1002. 421
- J. Lin, Woods Hole Oceanographic Institution, 266 Woods Hole Rd., 422
Woods Hole, MA 02543, USA. 423
R. S. Stein, U.S. Geological Survey, 345 Middlefield Rd., Menlo Park, 424
CA 94025, USA. 425
S. Toda, Disaster Prevention Research Institute, Kyoto University, 426
Gokasho Uji, Kyoto 611-0011, Japan. 427

Auxiliary Material Submission for Paper 2011GL047834

Widespread seismicity excitation throughout central Japan following the 2011 M=9.0 Tohoku earthquake, and its interpretation by Coulomb stress transfer

Shinji Toda (Disaster Prevention Research Institute, Kyoto University, Kyoto, Japan)

Ross S. Stein (U.S. Geological Survey, Menlo Park, California, USA)

Jian Lin (Woods Hole Oceanographic Institution, Woods Hole, Massachusetts, USA)

Geophys. Res. Lett., 38, doi:10.1029/2011GL047834, 2011

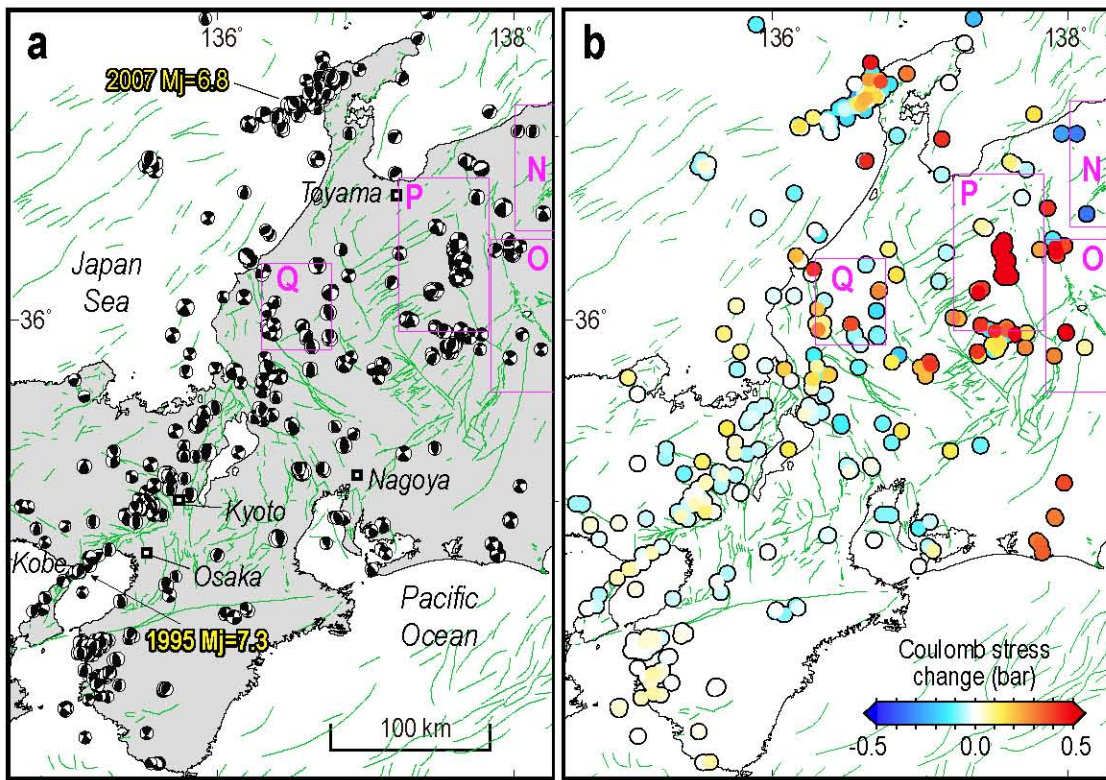
Introduction

This auxiliary material session contains three supplementary figures:

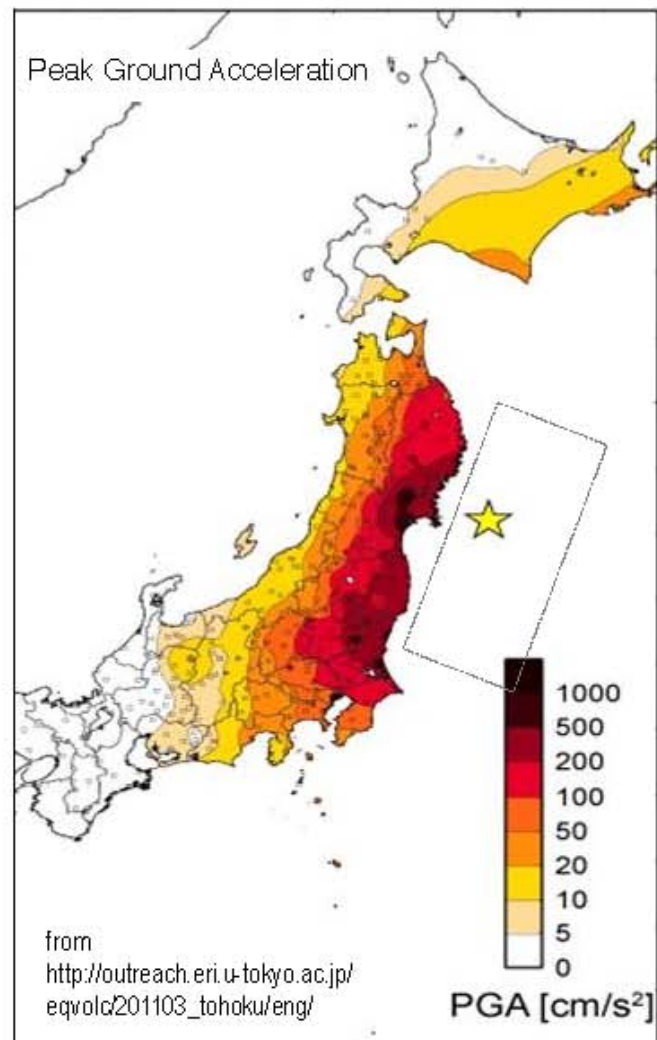
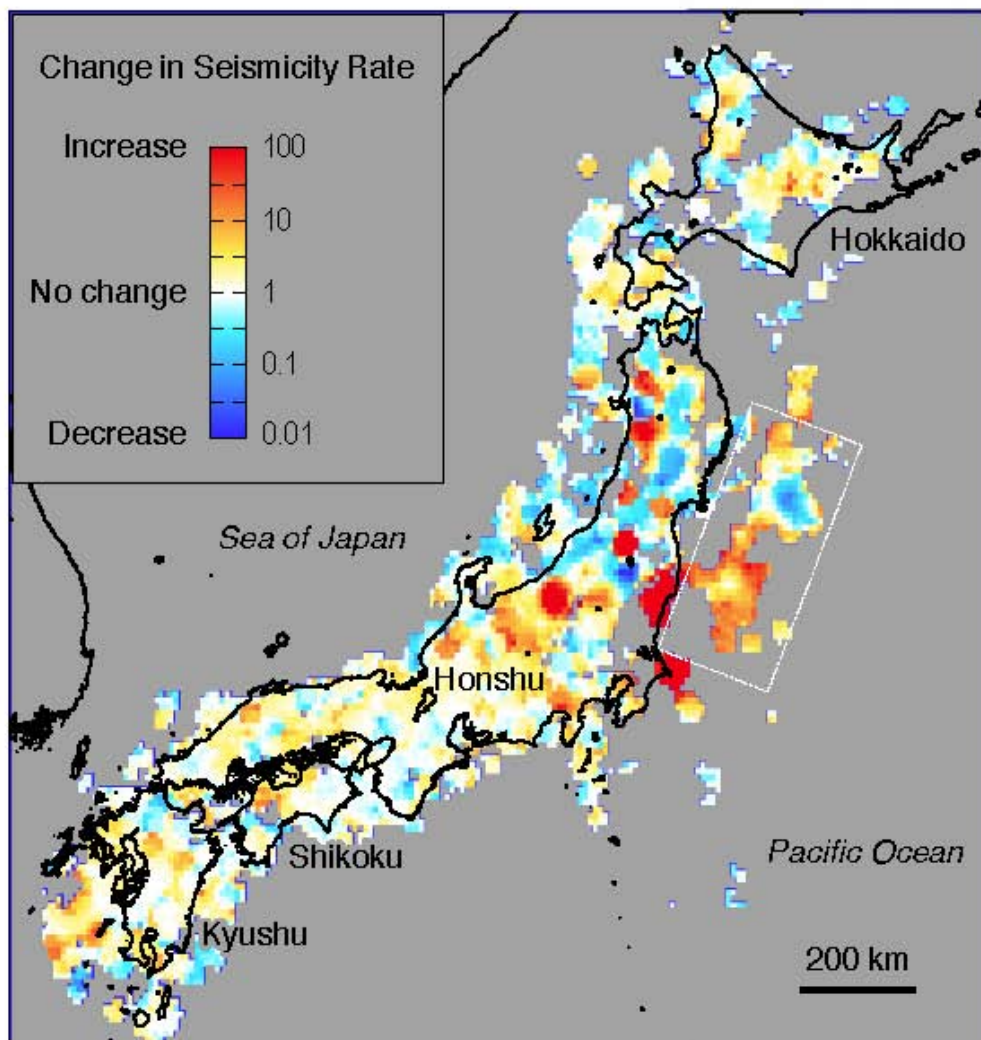
1. 2011GL047834R-fs01.eps (Supplementary Figure 1) Coulomb stress changes resolved on the nodal planes of the background earthquakes as proxies of local or regional fault structure in Chubu and Kinki districts. (a) Fault plane solutions since 1997 (depth ≤ 20 km). (b) Maximum Coulomb stress change from each pair of nodal planes.

2. 2011GL047834R-fs01.eps (Supplementary Figure 2) (Left panel) Seismic response of the entire Japan to the M=9.0 Tohoku mainshock for $M \geq 1.0$ seismicity (90 days post-mainshock compared to 1.2-years pre-mainshock), with a smoothing radius of 20 km, using the JMA PDE catalog downloaded on 10 June 2011. (Right panel) Peak ground acceleration recorded by the NIED K-NET/KiK-net strong motion seismographic network (open black squares). The observed seismicity rate changes are poorly correlated with the accelerations, suggesting that the dynamic stresses or intensity of shaking does not appear to control the seismicity response.

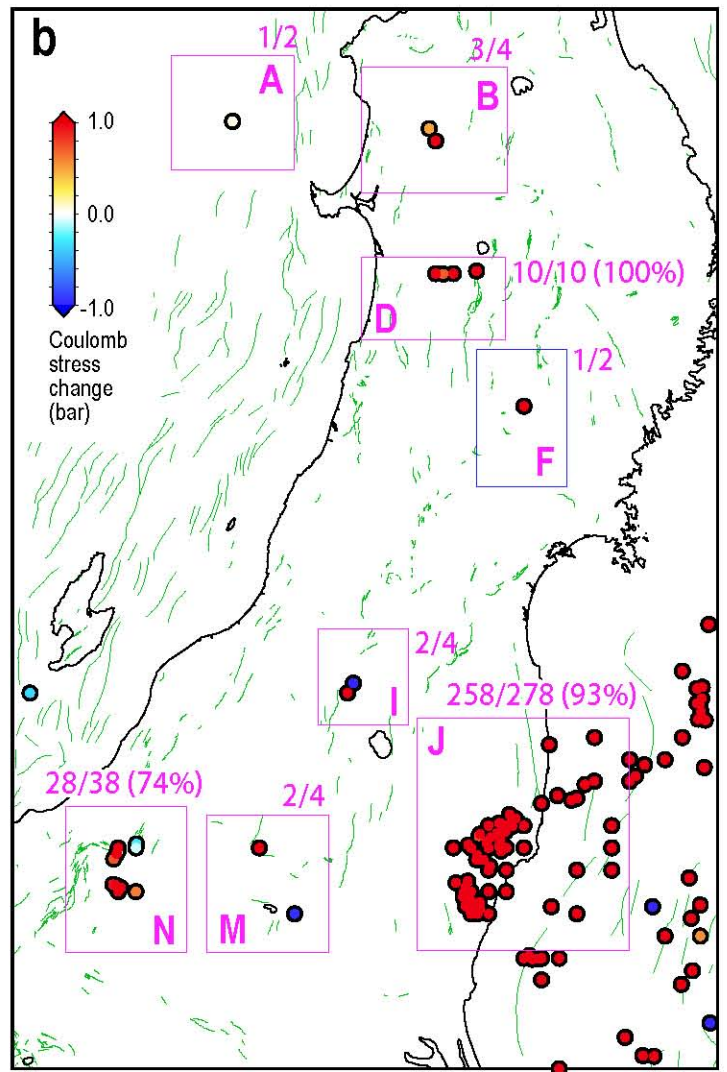
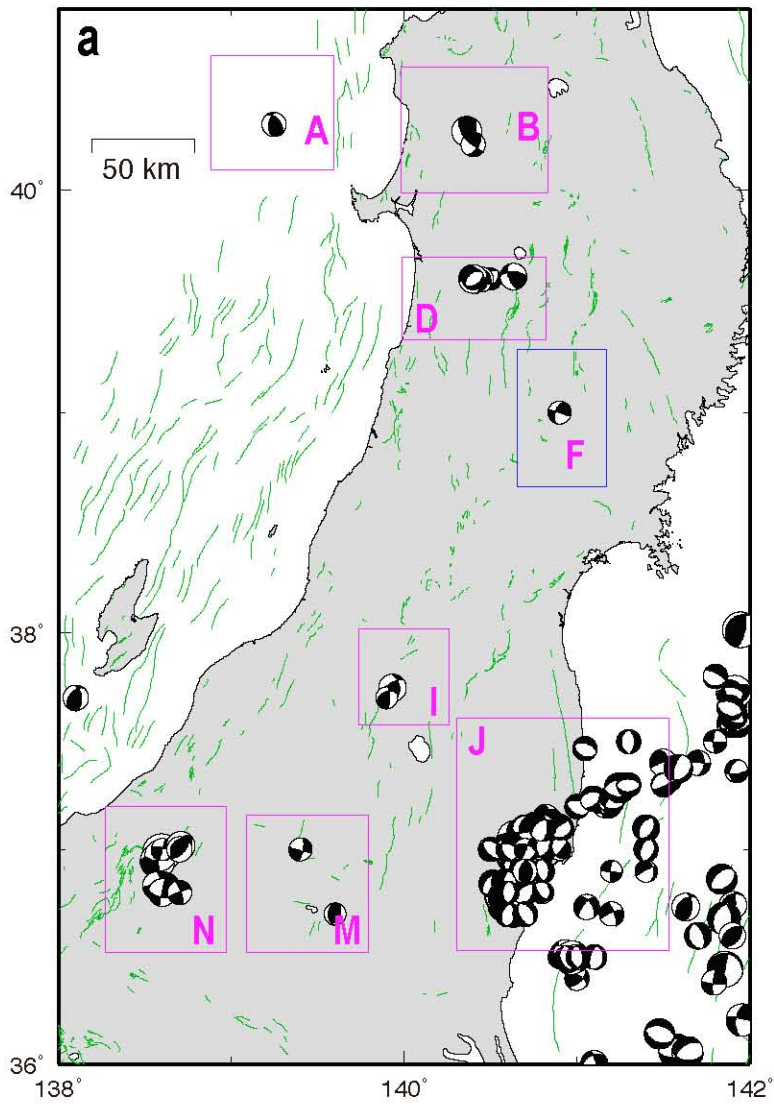
3. 2011GL047834R-fs01.eps (Supplementary Figure 3) Here we resolve the Coulomb stress change on the nodal planes of post-Tohoku earthquakes (11 March - 17 June 2011, depth ≤ 20 km) in the boxes which have either very few pre-Tohoku focal mechanisms, such as A, B, D, I, M, and N; or boxes in which the focal mechanisms after Tohoku profoundly changed (J, site of the 11 April 2011 Mw=6.7 Iwaki aftershock). Some 93% (258 out of 278) of the aftershocks in box J strike on nodal planes brought closer to Coulomb failure by the Tohoku mainshock.



Supplementary Fig. 1



Supplementary Fig. 2



Supplementary Figure 3